OPEN JOURNAL SYSTEMS
ISSN:2237-2202

Available on line at Directory of Open Access Journals
Journal of Hyperspectral Remote Sensing v.7, n.2 (2017) 91-100

www.periodicos.ufpe.br/revistas/jhrs

Journal of Hyperspectral Remote Sensing

Using Landsat-8 images in the estimative of surface radiation balance

Laurizio E. R. Alves[*], Ismael G. F. de Freita[**], Heliofábio B. Gomes[***], Fabrício D. dos S. Silva [****], Maurílio N. dos Santos [*****]

*Graduation student in Metereology, Atmospherical Science Institute / Federal University of Alagoas -UFAL, Maceió, Alagoas, laurizio.r@gmail.com (Corresponding author)
** Master student in Meteorology, Atmospherical Science Institute / UFAL, ismael.guidson@gmail.com;
***Professor Dr. in Metereology, Atmospherical Science Institute / UFAL, heliofab@gmail.com;
**** Professor Dr. in Meteorology, Atmospherical Science Institute / UFAL, fabricio.santos@icat.ufal.br;
***** Doctorate in Arquitecture, City Planning and Arquitecture College / UFAL, maurilioneemias2010@gmail.com.

Received 12 May 2017; accepted 4 August 2017

Abstract

The variation of the biophysical parameters is fundamental for the understanding of the dynamics of the land use and coverage in the estimation of the balance of surface radiation.In this context, the objective is to evaluate and validate the surface radiation balance for the Mogi Guaçu River Basin (MGRB) using Landsat-8 images and the Surface Energy Balance Algorithm for Land (SEBAL) algorithm. For the study used a Landsat-8 image orbits 220 and pointed 75 for the day 15/06/2015 and data from automatic stations Pradópolis and São Carlos (SP).The image processing was performed in the Qgis 2.18 software, where it performed the atmospheric correction (reflectance and radiance), then the albedo, temperature, emissivity, vegetation index, short wave and incident finally the radiation balance. The results showed that the dynamics of soil use and cover changes the final radiation balance, once the lowest values of albedo and temperature presented higher values of Normalized Difference Vegetation Index (NDVI) and Radiation balance, whereas higher values of albedo and temperature were noticed lower values of NDVI and Radiation Balance. The relative error obtained by the comparison of the measured and estimated radiation balance was around 4.35% showing the real accuracy of the Landsat-8 images for the estimation.

Keywords: Remote sensing, Biophysical parameters, Radiation balance.

1. Introduction

The products from orbital Remote Sensing is becoming an important tool to varied applications, particularly the ones related to the evaluation, handling, management, and administration of natural resources. It is also highlighted the importance of using this tool to analyze the alterations in the processes of mass transfer, heat, and moment, resulting from the modifications in the vegetal covering, aiming to obtain information that enables the generation of temporal and spatial series of the scenes in the study, facilitating the comparison among them. Besides allowing the determination of a direct form of biophysics parameters, energy, and radiation balance, without the necessity of knowledge of soil characteristics, and, of course, the agility in obtaining the update of estimated data and reduction of costs.

According to Santos et al. (2015) the balance of radiation has high relevance in the processes of air and soil heating, photosynthesis, and evapotranspiration, and it can be reckoned through the descendants, ascendants and radioactive fluxes, including the long and short waves. Silva et al. (2015) verified that different coverages of use and occupation of the soil alter the distribution of radiation balance, this way, the capacity of the surface in retaining energy to

the physic-biologic process and air heating are modified, consequently, altering the micro weather in all region.

The used algorithm *Surface Energy Balance Algorithm for Land* (SEBAL), proposed by Bastiaanssen (1995), has notability and it was used and validated in different areas (Gomes, 2009; Giongo, 2011), with the proposition of estimating the Evapotranspiration (ET) using orbital images and some surface data.

Rio Mogi Guaçu hydrographic basin (BHRMG) is located in the states of São Paulo and Minas Gerais, is at an average distance of 200 Km from the city of São Paulo, characterized by the presence of diverse industries and by the occupation of agricultural areas (sugar cane, mainly) in the border of the river (CBH-MOGI, 2015). BHRMG was selected to this study due to the different coverage, constituted by agriculture areas, woodsy pasture, urban mesh, etc. and from those characteristics, verify the influence of these different parts of the soil in the radiation balance to the surface.

In general, it is intended to know the variation of biophysics parameters that exist in the region of the hydrographic basin of the river Mogi Guaçu - SP, verifying the influence of the soil covering in the estimative of radiation balance to the service and check the accuracy of this estimative using the automatic seasons data to the validation. This way, to contribute for the modifications caused by the vegetation coverage and on the water loss on cultivated surfaces have more precise reviews, aiming to help the agriculture planning, management of hydric resources of a hydrographic basin, as well as, agriculturist, producers, civil society and the public power in the cultural administration.

2. Material and methodology

BHRMG has its main rivers: Mogi Guaçu river, Peixe river, and Jaguari-Mirim river. The basin is classified as industrial, highlighting the agro industry, vegetable oil and drinks, refrigerator and cellulose and paper industry. Prevailing agricultural activities of sugar cane, orange, pasture (brachiarium) and corn. It presents a coverage of approximately 10,5% of remnant natural vegetation, categories of significant occurrence are Semidecidual Seasonal Forest, Savanna, and the Tree/Shrub formation in regions of meadow. It presents an area of 14.463 Km^2, covering more than fifty cities in two states (São Paulo and Minas Gerais) and with a population of more than one million of people (SigRH, 2016).

Automatic stations

Automatic stations data collected to the date of the 10th of June 2015. Stations are located in the cities of Casa Branca – SP (Latitude: -21,78° and Longitude: -47,08°), Pradópolis – SP (Latitude: -21,34° and Longitude: -47,11°) and São Carlos – SP (Latitude: -21,98° and Longitude: -47,88°). In Figure 1 it is represented the distribution of the points of automatic stations of National Meteorology Institute (INMET) and the location of Mogi Guaçu hydrographic basin situated between the states of Minas Gerais and São Paulo, station data will serve to make the validation of balance estimative or surface radiation.

Acquisition and processing of orbital images

The acquisition of images from *Operational Land Imager* (OLI) e *Thermal Infrared Sensor* (TIRS) Landsat-8 sensors were made via https://earthexplorer.usgs.gov/, managed by *United States Geological Survey* (USGS). The used image corresponds the 220 orbit and points 75 to the 10th of June 2015.

Initially, it was made the treatment of the atmospheric correction and conversion of Digital Number (ND), shades of gray, in reflectance (USGS, 2016):

$$\rho_{\lambda,b} = \frac{H_\rho Q_{CAL} + A_\rho}{\cos(\theta_{SE})} \quad (1)$$

Where $\rho_{\lambda,b}$ is the monochromatic reflectance of all bands, H_ρ means specific multiplying re dimensioning of each band (constant value -0,1), A_ρ is the additive factor (constant value 2E-5), Q_{CAL} value pixel to pixel to each band (ND) and θ_{SE} azimuthal angle, that is calculated according to the following formula:

$$\theta_{SE} = 90 - \theta_{SZ} \quad (2)$$

Where: θ_{SZ} is the angle of the elevation of the sun, available on metadata.

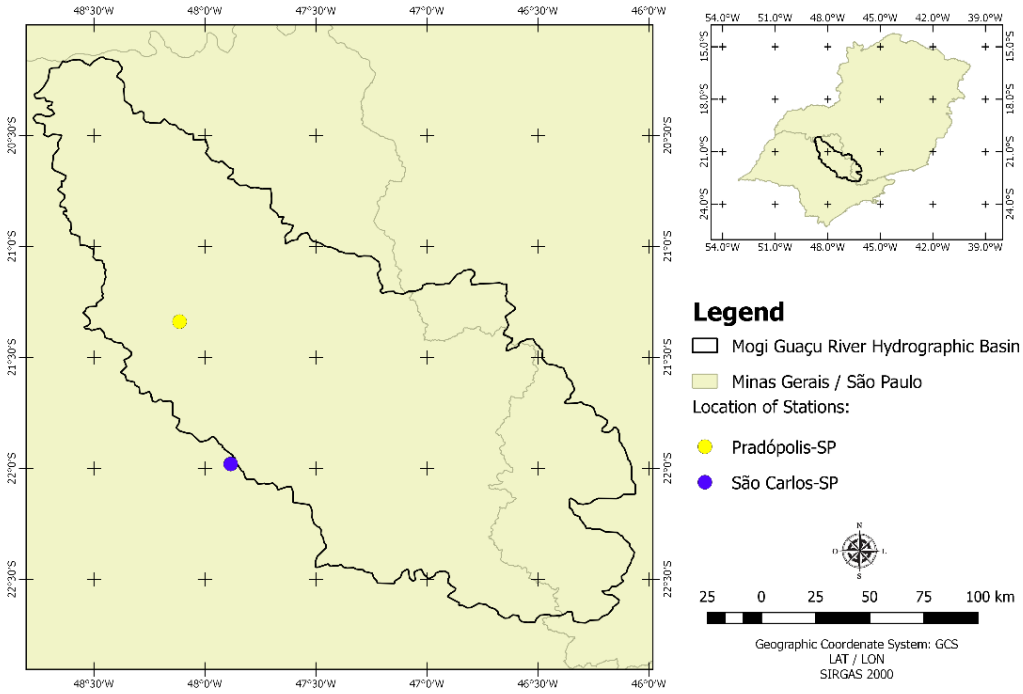

Figure 1 - Location of the Mogi Guaçu River Hydrographic Basin and spatial distribution of automatic stations.

Representing the albedo of the surface in the short wave radiation dominium (0,3 – 3,0 μm), however without atmospheric correction, being obtained through a linear combination of spectral reflectance $\rho_{\lambda,b}$, weighing $\varpi_{\lambda,b}$ stablished to each band, is the expression:

$$\alpha_{toa}=(\varpi 2*\rho_{\lambda,2})+(\varpi 3*\rho_{\lambda,3})+(\varpi 4*\rho_{\lambda,4})+(\varpi 5*\rho_{\lambda,5})+(\varpi 6*\rho_{\lambda,6})+(\varpi 7*\rho_{\lambda,7}) \quad (3)$$

In each weigh (ϖ2, ϖ3..., ϖ7) it is obtained by the reason between the specific constant solar of the band b and the sum of all the constant $ESUN_{\lambda,b}$, that is

$$\varpi_{\lambda,b} = \frac{ESUN_{\lambda,b}}{\sum ESUN_{\lambda,b}} \quad (4)$$

Where to the LANDSAT-8 the values are presented in the Table 1.

Table 1 - weigh coefficient (ϖn) to the planetary albedo calculation through the use of LANDSAT-8 images.

Bands	Band 2	Band 3	Band 4	Band 5	Band 6	Band 7
ϖn	0,300	0,277	0,233	0,143	0,036	0,012

Source: Silva et al. (2016).

Then it is made the albedo correction, is calculated according to the following equation, proposed by Tasumi et al. (2008):

$$\alpha_{sup} = \frac{\alpha_{TOA}-\alpha_{atm}}{\tau_{SW}^2} \quad (5)$$

Where α_{atm} is the portion of solar radiation reflected by the atmosphere, it was adopted 0,03 according to Bastiaanssen (2000) and τ_{SW} is the atmospheric transmittance to days with clear sky, Equation 6, proposed by Allen et al. (2002):

$$\tau_{SW} = 0{,}75 + 2 * 10^{-5} * Alt \quad (6)$$

Where *Alt* is the altitude of the used station (859 meters)

The calculations of the vegetation index are reckoned using the monochromatic

reflectance. The Normalized Difference Vegetation Index (NDVI), proposed by Tucker (1979), is obtained through the reason between the difference of infrared reflectance and infrared and the sum of the same reflectance, according to the equation (Allen et al., 2002):

$$IVDN = \frac{(\rho_{IV} - \rho_V)}{(\rho_{IV} + \rho_V)} \quad (7)$$

Where ρ_{IV} and ρ_V correspond, respectively, to the reflectance of infrared and red bands.

The Vegetation Index adjusted to the soil (IVAS), proposed by Huete (1988), this index aims to soften the ground effect;

$$IVAS = \frac{(1+L)(\rho_{IV} - \rho_V)}{(L + \rho_{IV} + \rho_V)} \quad (8)$$

Where L is a factor of soil adjustment, it was adopted L=0,5.

Then it is made the calculation of Leaf Area Index (IAF) that expresses the reason between the total area of leaves put in a particular pixel, by the area of the pixel, it is made by the calibrated empiric equation by Allen et al. (2002):

$$IAF = \frac{\ln\left(\frac{0,69 - IVAS}{0,59}\right)}{0,91} \quad (9)$$

After the IAF calculation, the Surface Emissivity is calculated (ε0) through inverted Plank's equation, proposed by a black body. The calculation of ε0 is made in function of IAF, as presented in the following equation:

$$\varepsilon_0 = 0,95 + 0,01 * IAF \quad (10)$$

To make the surface temperature calculation, before it has to be reckoned to the monochromatic radiance, using the band 10 from the *Thermal Infrared Sensor* (TIRS) LANDSAT-8. Applying the factors of re staggering of radiance given in the metadata (USGS, 2016):

$$L_\lambda = M_L Q_{cal} + A_L \quad (11)$$

Where; L_λ is the monochromatic radiance, ML is the fact of specific multiplicative re staggering ($3,342x10^{-4}$), AL is the factor of concrete additive re unbelievable (0,1), and Q_{cal} is the value pixel to pixel of the satellite image, through the Equation 11:

$$Ts = \frac{K_2}{\ln\left(\frac{K_1}{L_\lambda} + 1\right)} \quad (12)$$

Where K_2 e K_1 are constants of calibration of band 10, respectively 774,88K and 1321,08K.

Then, it is calculated the radiation of long wave emitted –$R_{ol,emi}$ ($W.m^{-2}$) by each pixel, through the equation of Stefan-Boltzmann, in the function of temperature Ts and the surface emissivity ε0:

$$R_{ol,emi} = \varepsilon_0 . \sigma . T_s^4 \quad (13)$$

In what σ is the constant of Boltzmann ($5,67*10^{-8}$ $W.m^{-2}.K^{-4}$).

Incident long wave radiation – $R_{ol,atm}$ ($W.m^{-2}$) is also calculated according to the equation of Stefan-Boltzmann, in the air emissivity function – ε_a and the air temperature – Ta (obtained by the station on the surface), given by:

$$R_{ol,atm} = \varepsilon_0 . \sigma . T_a^4 \quad (14)$$

In what:

$$\varepsilon_a = 0,85 . (-ln\tau_{sw})^{0,09} \quad (15)$$

The incident global solar radiation – Rs ($W.m^{-2}$) it is considered to the area of study and the lack of pyranometric data can be obtained according to the model (Allen et al., 2002; Gomes, 2009):

$$Rs = Q . cos\theta . dr . \tau_{sw} \quad (16)$$

Where Q is the solar constant (1367 $W.m^{-2}$); θ is the angle of solar incidence; dr is the distance Earth-Sun and τ_{sw} are the atmospherical transmissivities (calculated according to the equation 6).

The balance of the radiation Rn ($W.m^{-2}$) is obtained according to the following equation:

$$Rn=(1-\alpha).Rs+R_{ol,atm}–R_{ol,emi} – (1–\varepsilon_0).R_{ol,atm} \quad (17)$$

Where: α is the albedo surface; Rs is the radiation of incident short wave; $R_{ol,atm}$ is the radiation of incident long wave; $R_{ol,emi}$ is the radiation of emitted long wave, and ε_0 is the surface emissivity (4 – 100 μm).

Analyzes of orbital data

To the components analyze were highlighted four kinds of distinct soil coverage: Farming (sugar cane), woodsy pasture, urban mesh, and exposed soil. With the intention of verifying the variation of components from the radiation balance, Figure 2.

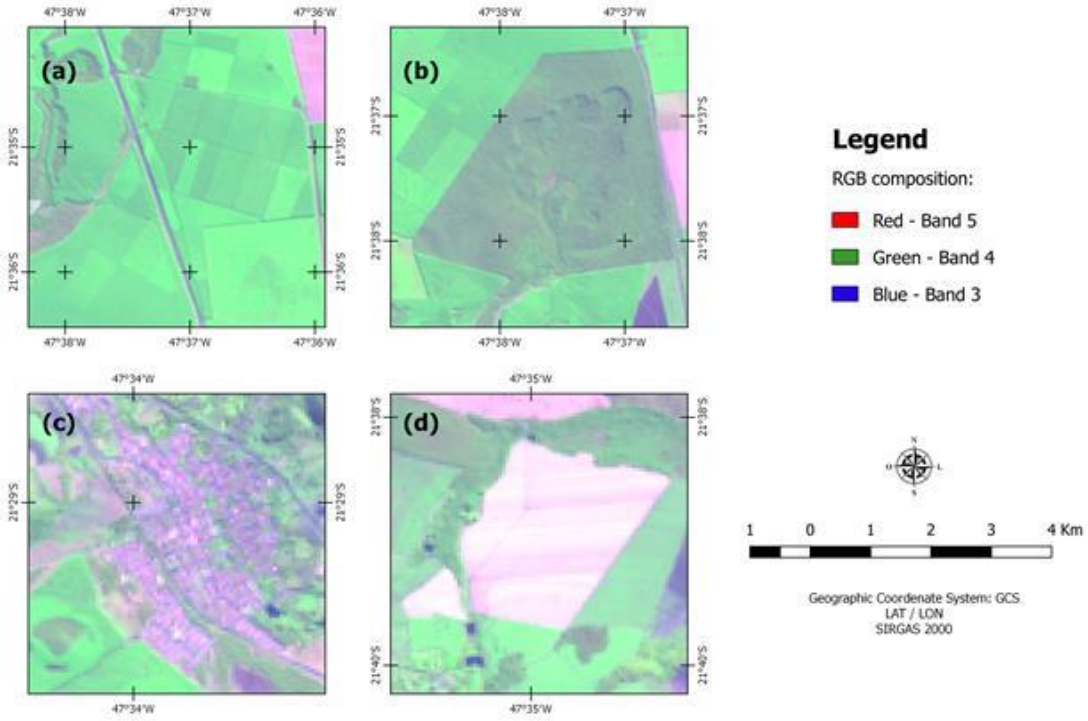

Figure 2 – RGB Composition (Red-band5, Green-band4, Blue-band3), featuring the four points: Farming (a), Woodsy pasture (b), Urban mesh (c) and exposed soil (d), 10/06/2015.

3. Results and discussion

In NDVI is observed that the higher values in the agriculture area, Figure 3 (a), superior to 0.615, because the lowest values were observed in the urban area, Figure 3 (c), lower zero values, that is attributed to the water bodies located at the Municipal Forest. Woodsy area, Figure 3 (b) presents NDVI values dominant in the band from 0.401 to 0.615. NDVI behaviour varies according to the strength of the vegetation and the hydric conditions, this way, healthy vegetation, nurtured of all its necessities, presents index higher values.

This behavior is based on the spectral signature from plants, that presents bigger absorption of solar radiation in the red region (band 4 of OLI sensor Landsat-8 – 0,85 – 0,88 μm) to convert this into energy resource in the process of photosynthesis, while plants present bigger reflectiveness in infrared (band 5 of OLI Landsat-8 sensor – 0,85 – 0,88 μm) as larger its strength can be. So, as bigger is its strength and nutrition, more elevated will be the absorption of red channel and the reflectiveness in the infrared channel (INSA, 2017). NDVI values are according to the literature, presenting values inferior to zero to water bodies, values next to zero to the urban areas and exposed soil, and higher values to the areas with higher vegetative density (Andrade, 2012; Alves et al., 2015; Freitas et al., 2016).

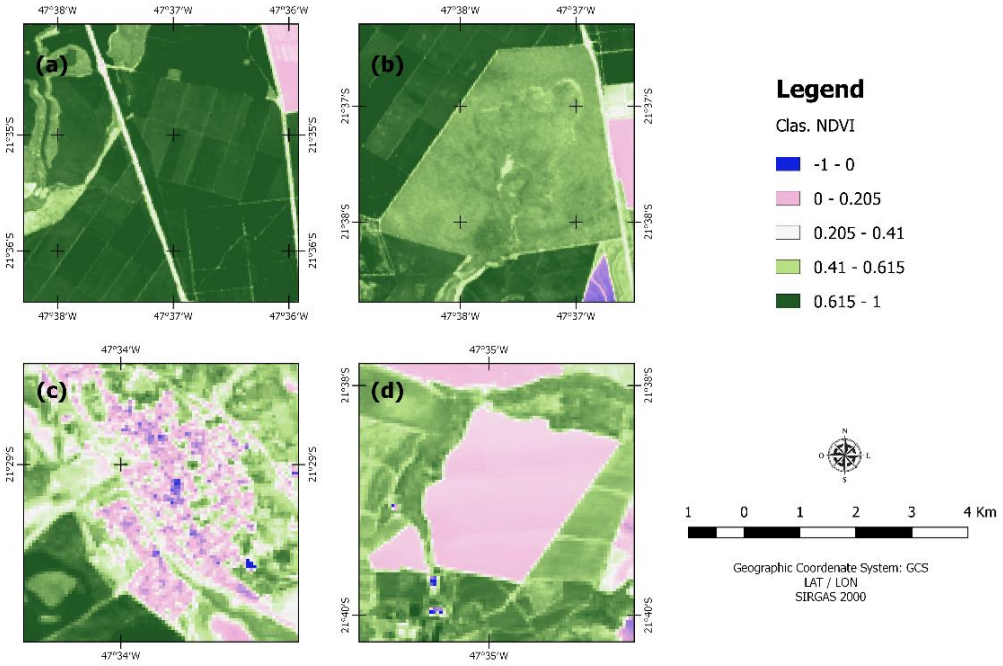

Figure 3 – Thematic map of NDVI obtained through OLI sensor Landsat-8, to the day 10/06/2015 to the BHRMG to the different coverage of soil: Agriculture (a), Woodsy pasture (b), Urban Mesh (c), Exposed soil (d).

The comparison of the NDVI and albedo values, Figure 4, it was observed that the areas with exposed soil (Figure 4(d)) and the urban area (Figure 4(c)), lower values of positive NDVI, present albedo superior the Figure 4 (a) and (b). so, the alteration of use and soil coverage, substitution of the vegetated area by urban area or bare land, implicates in changes in the albedo that, consequently, will affect the final balance of radiation and energy. This way, contributing to the increase of thermic sensation, high surface temperature, as it is observed in Figure 5 (a) and (d), for example.

These alterations in albedo values are due to the fact that the reflective characteristics of soil constituents are altered, this way, changing the angle of incidence of solar ray. Besides that, solar radiation that gets the vegetation is converted into energy contributing to the photosynthesis process, at the same time, this radiation that incurs in the vegetation in urban area and naked soil is not used in any physic biologic process, contributing only to the increase of the temperature of constituents with no vegetation (buildings, roofs, asphalt, etc.).

According to Pereira et al. (2012) in the study made in Barra dos Coqueiros basin (Goiás), authors highlight that areas recovered by vegetation presented lower temperature than areas with exposed soil. Andrade et al. (2012) highlights that the small values of NDVI found to the urban mesh of Santarém-PA, is associated with the increase of reflection of the aims (buildings, houses, paved streets, buildings), that is evidenced by the increase of albedo and temperature, the same occurs with exposed soil area. The results of these authors agree with what was observed in this study.

As it was checked by the analyze of thematic maps of NDVI, albedo and temperature, the use and occupation of soil alters the thermo regulator mechanism of the environment. These alterations generate the micro weathers that can change the local pluviometrical regime, as well as to increase the temperature, besides changing the radiation balance (Rn). As it was observed when the vegetation area is checked (Figure 5(b)) with temperature varying between 18 and 19,5 °C and urban areas (Figure 5 (c)) that can present higher superior to 22,5°C generating an increase of local temperature around 3 °C.

When comparing the found values of surface temperature between green areas and urban areas it is evident the influence of compactness and construction of the urban mesh in micro weather because the alteration of this kind of coverage provoked the increase of temperature around 3 °C. According to Gartland (2011) there are two main reasons for this warming, the construction of urban mesh

covered by impermeable soil, and therefore, there is no available humidity to dissipate the heat, and the combination of dark material in edification retain more solar energy. In dark and dry (urban) areas are presented higher temperature than vegetated surfaces and wet surfaces.

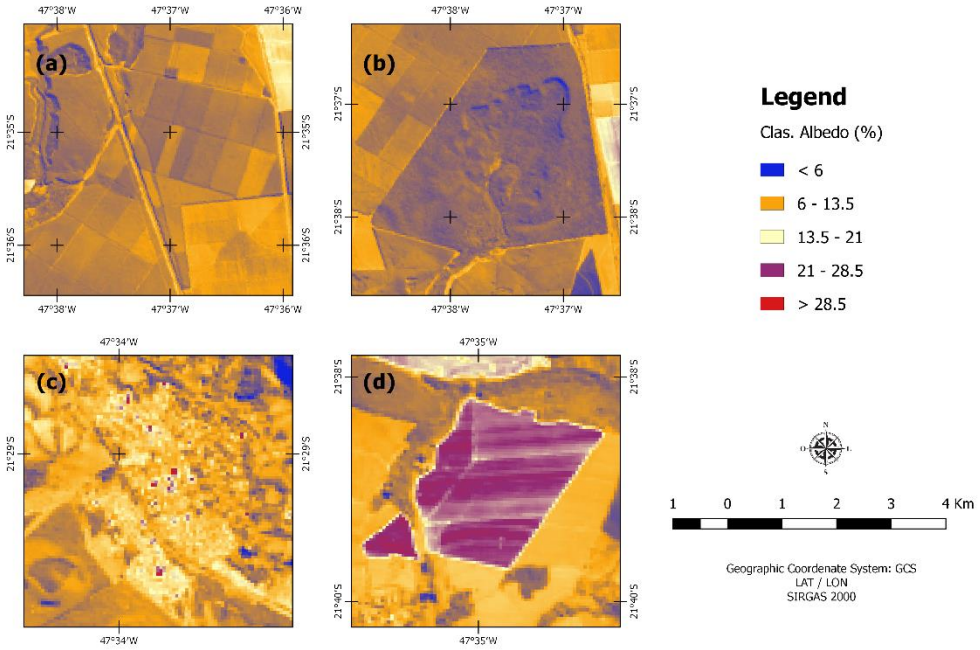

Figure 4 – Thematic map of surface Albedo obtained through the OLI sensor Landsat-8, to the day 10/06/2015 to the BHRMG to the different soil coverage: Agriculture (a), woodsy pasture (b), urban mesh (c), exposed soil (d).

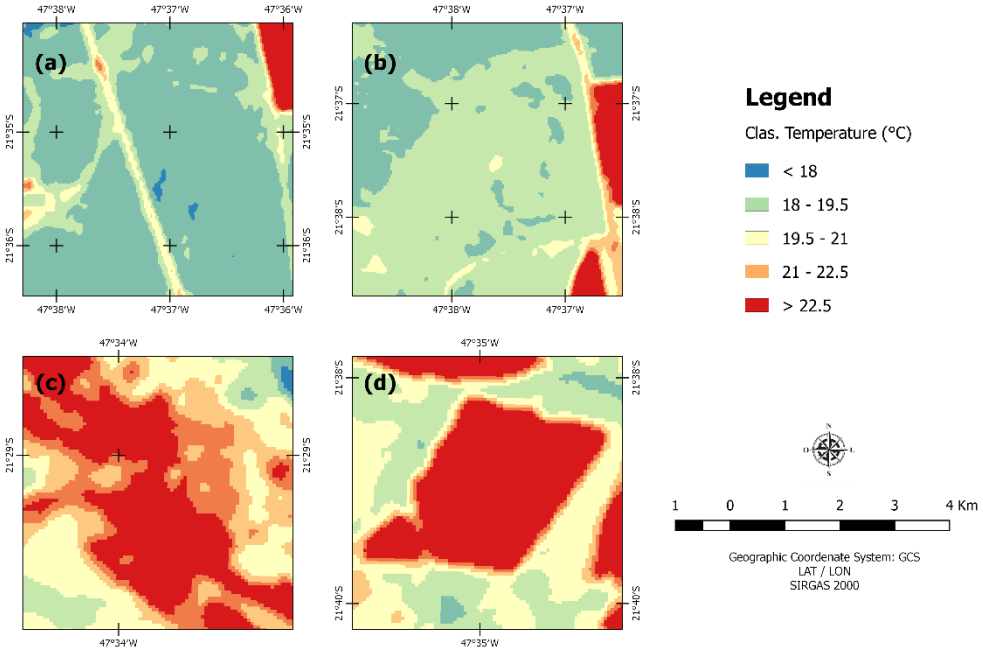

Figure 5 – Thematic map of the temperature of the surface obtained by the OLI sensor Landsat-8, to the day 10/06/2015 to the BHRMG to the different coverage of soil: Agriculture (a), woodsy pasture (b), urban mesh (c), exposed soil (d).

Figure 6 presents the values of Rn estimated from the model SEBAL and images of OLI/TIRS sensor Landsat-8 to the day 10/06/2015. We can verify that the lower values of Rn are observed in urban areas and exposed soil, Figure 6 (c) and (d), and these areas present

high albedo, because the higher values of Rn is observed to the Figure 6 (a) and (b), agriculture, woodsy pasture, respectively, in which is observed the lowest albedo values, this results corroborate with the ones found by Gomes (2009) that verified high values of Rn associated with the areas with low albedo and Fausto (2014) that tested that "the substitution of woodsy pasture by agronomic cultures in the south of Mato Grosso has impacted the decrease of available energy to the surface, represented by the radiation balance". These factors imply that the substitution of the coverage will have as a consequence alteration on local micro weather, and as these alterations present bigger coverage it will able to implicate in changes in a larger scale than the local weather.

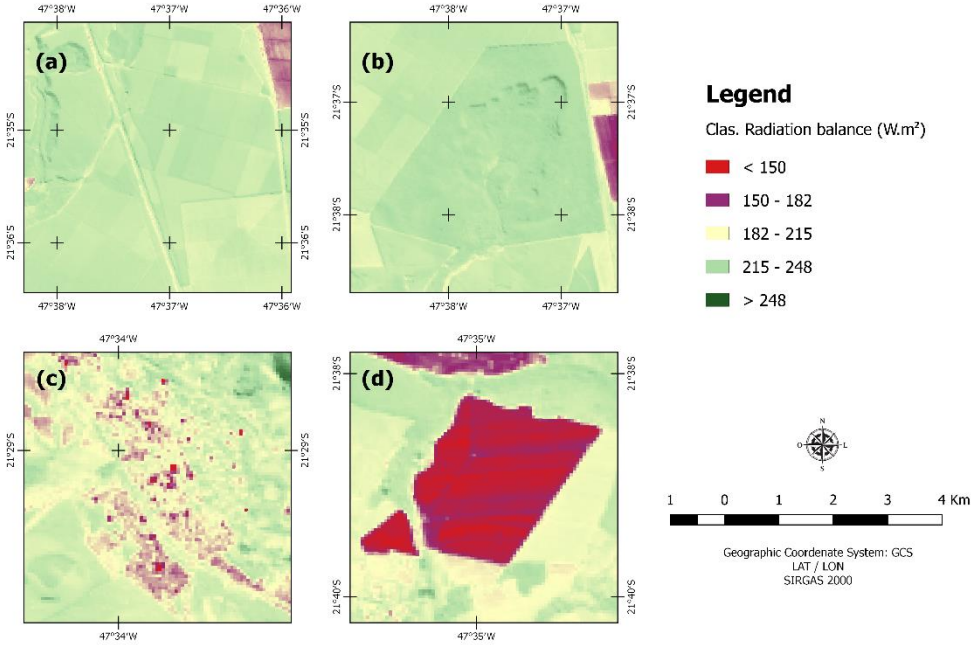

Figure 6 – thematic map of radiation balance to the surface obtained through the OLI sensor Landasat-8, to the day 10/06/2015 to the BHRGM to the different coverage of soil: Agriculture (a), woodsy pasture (b), urban mesh (c), exposed soil (d).

In Table 2 there are represented the instantaneous values of radiation balance obtained by SEBAL and images of OLI/TIRS sensor Landsat-8 and the data measured by the automatic stations of INMET. The presented results are for the day 28/06/2016 and the value of Rn between two points present variation of 9,00 W.m-2, in which we can observe that therefore spatialization of points the estimated values are close to the measured values. In which the balance amounts of radiation the estimated surface very a bit in relation to the measured data, presenting a relative error of 4,35%. It is emphasized that the chosen altitude to the calculation of transmissivity was São Carlos- SP one that showed lower error (0,34%), while the estimative of Pradópolis – SP that presented higher error, attributed to the station altitude. However, due to the excellent accuracy of estimative between two locations be inferior to 10%, it showed that the use of Landsat-8 images to the estimative of radiation balance presented an acceptable error.

This way, it is suggested that the estimative Rn from the Landsat-8 images show a good accuracy, admitting a relative error lower than 10%, this methodology can be well used in areas where the automatic stations do not exist, representing a result of high importance and practical utility.

These results reinforce previous studies related to the precision of Landsat images, as a study made by Gomes (2009) that validated the estimated Rn to the Mogi Guaçu basin to the coverage of woodsy pasture, and sugar cane using Landsat-5 images obtaining errors to the images inferior to 10%.

Table 2 – radiation balance values to the surface - – Rn ($W.m^{-2}$) obtained by SEBAL and measurements of automatic stations, with their respective relative errors.

Automatic Stations	Estimated ($W.m^{-2}$)	Measured ($W.m^{-2}$)	Error (%)
Pradópolis –SP	201,9	220,29	8,35
São Carlos – SP	211,0	211,72	0,34
		Average error (%)	4,35

4. Conclusion

The variety of soil coverage implicated in bio physic parameter alteration and, consequently, in final radiation balance. Different coverage showed on Normalized Difference Vegetation Index (NDVI) revealed that the various constituents show different abilities of radiation retention and reflection, this way, implicating in alterations in the estimated variables of surface albedo and the surface temperature. It is highlighted that through the analyze of the surface temperature map it was possible to identify the behaviour of urban heat islands, where the urban mesh presented a temperature superior to 3°C in relation to the surroundings (areas with vegetation).

Besides that, in map analyzes it was evident that the different coverages influence in the radiation balance to the surface, while the vegetated areas present higher availability of radiation (radiation balance), while urban areas and bare soil current low availability of radiation.

Landsat-8 images showed a relative average error inferior to 5% in the estimative of radiation balance to the surface. Soon, the application of SEBAL algorithm against the Landsat-8 images makes great tools to the estimative of these parameters and consequently becomes an alternative to the areas that do not present a proper distribution of the stations. Contributing to a better understanding of radiation and to soil coverage dynamic and it can be applied to the agricultural planning, urban and monitoring of bio physics parameters.

Acknowledgments

The first author thanks the Foundation of Support to the Research of Alagoas State (FAPEAL), by the concession of scientific research scholarship.

The authors thank the Meteorology National Institute (INMET) for ceding the data of the automatic stations.

References

Allen, R.G., Tasumi, M., Trezza, R., 2002. SEBAL (Surface Energy Balance Algorithms for Land). Advanced Training and User's Manual – Idaho Implementation, version 1.0, 97.

Alves, L.E.R., Gomes, H.B., Santos, M.N., Ocrecio, T.C.M., Nascimento, G.C., Peixoto, I.P., 2015. Métodos para obtenção e análise do albedo de superfície e NDVI, para o município de Triunfo - PE. Simpósio sobre Geotcnologias e Geoinformação do Estado de Alagoas, Maceió.

Andrade, R.G., Sediyama, G.C., Paz, A.R., Lima, E.P., Facco, A.G., 2012. Geotecnologias aplicadas à avaliação de parâmetros biofísicos do Pantanal. Pesquisa Agropecuária Brasileira 47,1227-1234.

Bastiaanssen, W.G.M., 1995. Regionalization of surface flux densities and moisture indicators in composite terrain: a remote sensing approach under clear skies in Mediterranean climates. Thesis (Master). Wageningen, WUR. Available: http://library.wur.nl/WebQuery/wurpubs/fulltext/206553. Access: mar, 16, 2017.

Bastiaanssen, W.G.M., 2000. SEBAL-based sensible and latent heat fluxes in the irrigated Gediz Basin.Turkey. Journal of Hidrology 229, 87-100.

CBH-MOGI. Comitê da Bacia Hidrográfica do Rio Mogi Guaçu, 2015. Plano da Bacia Hidrográfica do Rio Mogi Guaçi 2016-2019. Available: http://www.sigrh.sp.gov.br/public/uploads/documents/9069/diagnostico_sintese_cbh-mogi.pdf. Access: mar, 22, 2017.

Fausto, M.A., 2014, Análise de parâmetros biofísicos estimados pelo algoritmo SEBAL em áreas de Cerrado na bacia do alto rio Paraguai, Dissertation (Master). Cuiabá, UFMT.

Freita, I.G.F., Gomes, H.B., Moura, M.A.L., Alves, L.E.R., Silva Júnior, J.R., Santos, M.N., 2016. Estudo dos índices de vegetação e temperatura em anos de El Niño para o município de Cabrobó-PE com uso de imagens de satélite. Simpósio sobre Geotcnologias e Geoinformação do Estado de Alagoas, Maceió.

Gartland, L., 2011. Ilhas de calor: como mitigar zonas de calor em áreas urbanas. Oficina de Textos, São Paulo.

Gomes, H.B., 2009. Balanço de radiação e energia em áreas de cultivo de Cana-de-açúcar e Cerrado no Estado de São Paulo mediante imagens orbitais. Thesis (Doctoral). Campina Grande, UFCG.

Giongo, P.R., 2011. Mapeamento do balanço de energia e evapotranspiração diária por meio de técnicas de sensoriamento remoto. Thesis (Doctoral). Esalq-USP, Piracicaba.

Huete, A.R.A., 1988. Soil-Adjusted Vegetation Indes (SAVI). Remote Sensing of Environment 25, 205-309.

INSA. Instituto nacional do Semiárido, 2017. NDVI – parceria INSA e LAPIS/UFAL. Available: http://www.insa.gov.br/ndvi#.WNJ_kPnyu70. Access: mar, 22, 2017.

Pereira, C.C., Mariano, Z.F., Wachholz, F., Cabral, J.B.P., 2012. Análise da temperatura de superfície e do uso da terra e cobertura vegetal na bacia dos Coqueiros (Góias). Revista Geonorte 2, 1243-1255.

Santos, F.A.C., Santos, C.A.C., Araújo, A.L., Cunha, J.E.B., 2015. Performance of methodologies for estimating Net radiation from Modis images. Revista Brasileira de Meteorologia 30, 295-306.

Silva, L.C., Cunha, J.M., Machado, N.G., Campos, M.C.C., Biudes, M.S., 2015. Estimativa do balanço de radiação por sensoriamento remoto de diferentes usos de solo no sudoeste da Amazônia brasileira. Revista Sociedade & Natureza 27, 341-356.

Silva, B.B.da, Braga, A.C., Braga, C.C., Oliveira, L.M.M.de, Montenegro, S.M.G.L., Barbosa Junior, B., 2016. Procedures for calculation of the albedo with OLI-Landsat 8 images: application to the Brazilian semi-arid. Revista Brasileira de Engenharia Agrícola e Ambiental 20, 3-8.

SigRH. Sistema Integrado de Gerenciamento de Recursos Hídricos do Estado de São Paulo, 2016. Available: http://www.sigrh.sp.gov.br/cbhmogi/apresentacao. Access: mar, 21, 2017.

Tasumi, M., Allen, R.G., Trezza, R., Wright, J.L., 2008. Satellite-based energy balance to assess within – population variance of crop coefficient curves. Journal of Irrigation and Drainage Engineering ASCE, 94-108.

Tucker, C.J., 1979. Red and photographic infrared linear combinations for monitoring vegetation. Remote Sensing of Environment 8, 127-150.

USGS. United State Geological Survey, 2016. Using the USGS Landsat 8 Product. Available: https://landsat.usgs.gov/using-usgs-landsat-8-product. Access: mar., 25, 2017.